

# Geometrical Frustration and Static Correlations in a Simple Glass Former

Benoît Charbonneau,<sup>1</sup> Patrick Charbonneau,<sup>2,3</sup> and Gilles Tarjus<sup>3</sup>

<sup>1</sup>*Mathematics Department, St. Jerome's University in the University of Waterloo, Waterloo, Ontario, Canada*

<sup>2</sup>*Departments of Chemistry and Physics, Duke University, Durham, North Carolina 27708, USA*

<sup>3</sup>*LPTMC, CNRS-UMR 7600, Université Pierre et Marie Curie, boîte 121, 4 Place Jussieu, 75252 Paris, France*

(Dated: August 11, 2011)

We study the geometrical frustration scenario of glass formation for simple hard spheres systems, and find it to be an inefficient description. The possibility of a growing static length is furthermore found to be physically irrelevant in the simulation accessible regime, which suggests that the study of any structural order in simple fluids of spherical particles is there also unhelpful.

PACS numbers: 64.70.Q-, 64.70.kj, 61.20.Ja, 02.40.Dr

Glass formation and jamming are ubiquitous phenomena observed in a variety of molecular and colloidal systems. Identifying a relevant amorphous order parameter that captures these materials' rich phenomenology remains, however, a challenge. Several theoretical approaches emphasize the role of a growing static length associated with the glassy dynamical slowdown, and proposals for growing structural correlations in supercooled liquids have recently flourished. Detecting static correlations by "order agnostic" approaches is a promising avenue [1–3], but it intrinsically limits geometric insights into the underlying microscopic mechanism. A scenario for growing geometrical order proposed some time ago by Sadoc and Mosseri [4] as well as by Nelson and coworkers [5] has had a marked impact on the analysis of the structure of dense fluids. In addition to encouraging the enumeration of preferred local structures, e.g., [6], the proposal has also led to the development of a theoretical apparatus for the glass transition based on geometrical frustration [5, 7]. Although it also provides a geometrical interpretation for the "hidden" static correlations, the theory remains largely untested in three-dimensional (3D) systems.

Geometrical frustration is canonically illustrated by considering the behavior of spherical particles with diameter  $\sigma$ . Because regular simplices (triangles in 2D, tetrahedra in 3D, etc.) are the densest possible local packing of spheres, they are expected to play a central role in liquid organization, e.g., [8, 9]. In 2D Euclidean space, interesting physics results from the fact that simplices can assemble into the triangular lattice [5], and spatial curvature frustrates the regular assembly of disks [10]. For Euclidean space in dimension  $d \geq 3$ , however, simplices cannot tile space without defects. Yet a regular tiling of tetrahedra is found on the sphere that inscribes the remarkably large 4D platonic polytope  $\{3, 3, 5\}$ . The inscribing sphere's curvature  $R^{-2} = \pi^2/(25\sigma^2)$  is much smaller than  $R^{-2} = \pi^2/(4\sigma^2)$  for the generalized octahedron  $\{3, 3, 4\}$ . On the sphere with  $d > 3$ , by contrast,  $\{3^{d-1}, 4\}$  is the only way to obtain a regular tiling of simplices resulting in large geometrical frustration of the corresponding Euclidean space [11], which hints at

a singular role for simplex ordering in 3D. The defects that result from uncurving  $\{3, 3, 5\}$  can be understood by dimensional analogy. Each particle in a perfect 2D triangular tiling of disks is part of six simplices. Curvature results in irreducible disclinations that sit on disk centers and for which the coordination obtained by a Delaunay decomposition differs from six. Similarly, in 3D each edge between nearest-neighbor pairs within  $\{3, 3, 5\}$  is shared by five other tetrahedra; flattening space generates disclination lines of "bond spindles" that are shared by  $q \neq 5$  tetrahedra. Periodic arrangements of these disclinations form the complex crystal structures known as Frank-Kasper phases [12]. Yet even in amorphous configurations *at small frustration*, the simple Voronoi polyhedra that accommodate the presence of spindles with  $q \neq 5$  provide topological constraints for the propagation of defects from one particle to the next [5]. For example, a spindle with  $q = 4$  (or  $q = 6$ ) can only propagate, spread, or be terminated by a pair of  $q = 6$  ( $q = 4$ ) spindles. A denser fluid, in which the proportion of  $q = 5$  spindles grows (and conversely that of  $q \neq 5$  spindles shrinks), should thus see disclination defects play a more important role. Disclination lines passing one another correspond to activated events, possibly affected by topological constraints [5]; the more extended these defect lines become, the slower the relaxation. The theoretical framework therefore suggests a causality between the dynamical slowdown and a growing static, structural correlation length underlying the fragility of the glass-forming fluid. In this letter, we critically examine this proposal and find that, in spite of its elegance, it does not hold for the system to which it is more directly related, i.e., simple 3D hard spheres. Through a variety of measures of static order, we also consider alternate definitions of correlation lengths and explore in what regime a growing static order could reasonably be associated with a dynamical slowdown.

Testing this intrinsically geometrical theory on identical 3D hard spheres is problematic, because nucleation interferes with the dynamical slowdown. We thus consider two perturbations that reduce the crystallization drive, in case the fluid structure were to sensitively de-

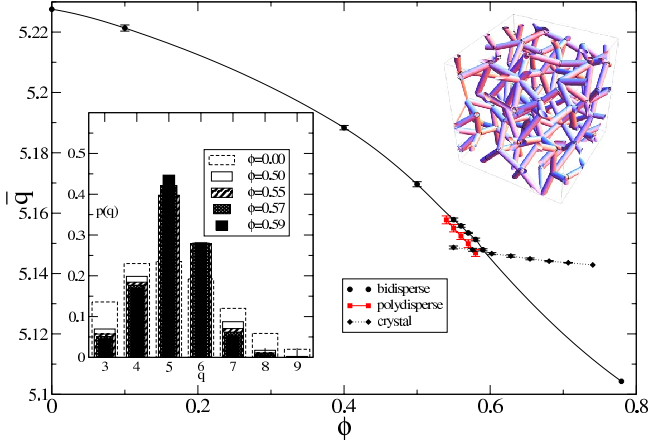


FIG. 1: Evolution of  $\bar{q}$  and (left inset) of the probability distribution  $p(q)$  with density. The statistical honeycomb  $\{3, 3, \bar{q}\}$  limit is given for reference. (right inset) Network of  $q = 6$  spindles (rods) at  $\phi = 0.58$ .

pend on the nature of the perturbation: (i) a 50:50 binary mixture with a 1.4:1 diameter ratio whose glass-forming properties have been extensively characterized [13–15], and (ii) a system of hard spheres with the smallest non-crystallizing diameter polydispersity, 8.5% [16]. The average number of tetrahedra wrapped around a bond,  $\bar{q}$ , lies within two simple limits. On the one hand, all finite-density configurations should have fewer tetrahedra per spindle than a Poisson process (an ideal gas), where  $\bar{q} = 144\pi^2/(24\pi^2 + 35) \approx 5.228$  [17]. On the other hand, although in curved space the optimal number of simplices per bond can be as low as  $q = 5$ , in Euclidean space a more stringent limit  $\bar{q} = 2\pi/\arccos(1/3) \approx 5.104$  is obtained from the fictitious “statistical honeycomb” polytope  $\{3, 3, \bar{q}\}$  [18]. Figure 1 shows that the densifying fluids do present a growing polytetrahedral character. The average spindle coordination decreases, seemingly toward its optimal value, with increasing packing fraction  $\phi$  for both models, as does its distribution  $p(q)$  (Fig. 1). The growing simplex order is also quite different from that observed in the face-centered cubic crystal phase. Because the structural properties of the two models are robustly similar, we only consider (i) for the rest of the analysis.

Surprisingly, even for the densest systems equilibrated the disclination network remains highly branched, with multiple defect lines stemming from each vertex. The inset of Fig. 1 illustrates this situation for the  $q = 6$  spindle network. The typical spacing between defect spindles  $\xi_{\text{defect}} \equiv c_{\text{defect}}^{-1/3}$ , using a defect concentration  $c_{\text{defect}} \equiv \sum_q c_q(q-5)^2$  that puts more weight on higher-order defects, indeed grows by no more than 1–2% over a density range over which the relaxation time goes up by several decades. Extrapolating the results to higher densities using the statistical honeycomb limit further suggests that the growth of  $\xi_{\text{defect}}$  remains small over

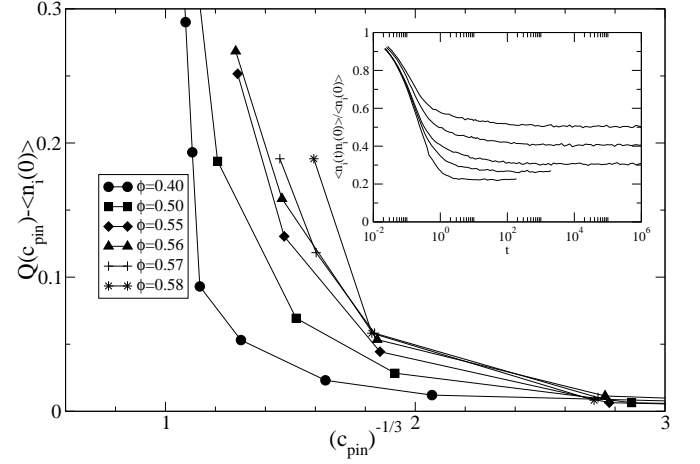


FIG. 2: Long-time limit of the overlap. (inset) Time  $t$  evolution of the overlap for  $c_{\text{pin}} = 0.11, 0.45, 0.68, 0.74$ , and  $0.79$ , from left to right, in  $\sqrt{\beta m \sigma}$  units with mass  $m$ , the larger particle  $\sigma$  and inverse temperature  $\beta$  set to unity.

the entire accessible amorphous regime  $\phi \lesssim 0.65$ . Actually, polytetrahedral order is bound to saturate as a result of the intrinsic frustration of Euclidean space. The saturation length corresponding to the maximal spatial extension of simplex order estimated from the radius of the sphere inscribing  $\{3, 3, 5\}$  is  $R \simeq 1.59\sigma^2$ . Alternatively, the typical distance between defects in an ideal tetrahedral structure threaded only by  $q = 6$  spindles is  $\xi_{\text{defect}} \simeq 0.99\sigma$ , noting that the average distance between spindles itself is  $\approx 0.3\sigma$ . A small distance between defects is not necessarily indicative of a small structural correlation length because  $q = 5$  order already percolates. Yet the shear quantity of defects and the relatively stable  $c_{\text{defect}}$  suggest that if a static length exists, it is unlikely to change much at these high densities. A similar result is obtained for the spatial correlations associated with frustrated local order through an analysis of the spatial decay of the bond-orientational order correlation function  $G_6(r)$  [19, 20]. No matter how it is precisely defined, the associated correlation length  $\xi_6$  does not increase by more than a few percents. Hard-sphere systems are thus sufficiently frustrated even in 3D to make the dual picture of amorphous particle packings in terms of spindle defects rather uneconomical.

In order to remove any possible doubt as to whether alternative static lengths due to tetrahedral or other order types are present or not, we turn to the order-agnostic penetration length  $\xi_p$  [21, 22], which, like the point-to-set length  $\xi_{\text{PS}}$  [1], characterizes the influence of boundary conditions. It is obtained by pinning a random selection of particles from an equilibrated fluid configuration, and measuring the overlap between the initial and final configurations after a long time  $t$  has elapsed,

$$Q(c) = \lim_{t \rightarrow \infty} \frac{\sum_i \langle n_i(0)n_i(t) \rangle}{\sum_i \langle n_i(0) \rangle}, \quad (1)$$

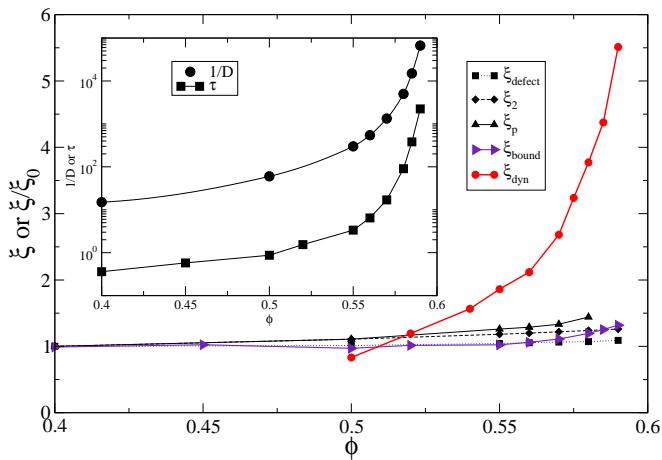


FIG. 3: Various static lengths rescaled to unity at  $\phi = 0.40$  ( $\xi_0$ ) together with the lower bound from Eq. (2)  $\xi_{\text{bound}}$  and the dynamic length [14]. (inset) Measures of dynamical slowdown. Lines are guide for the eyes.

where  $n_i$  is the occupancy of a spatial cell whose volume is similar to that of the smaller particles in the system in order to prevent multiple occupancy [21]. Subtracting the random overlap contribution  $\langle n_i \rangle$  leaves a quantity that grows from low to high as the pinning concentration  $c_{\text{pin}}$  increases (Fig. 2); the crossover is  $\xi_p \sim c_{\text{pin}}^{-1/3}$ . Operationally, we define  $\xi_p$  as the value of the average distance for which the overlap falls below 0.18 (Fig. 2). The extracted length is not very sensitive to this choice, provided it is intermediate between low and high overlap. We stress that focusing solely on the low-overlap regime provides no information on  $\xi_p$  as it only depends on the standard pair correlation function and therefore on trivial two-point correlation lengths  $\xi_2$ . This result, which can be checked explicitly by considering the linear response to a vanishingly small concentration of pinned particles, remains true so long as one remains in the low overlap perturbative regime [23]. It also casts some doubt on the relevance of a recently proposed scaling [24], where the observed linear dependence on concentration suggests instead that only trivial static lengths are probed.

Figure 3 shows that the penetration length  $\xi_p$  increases only very modestly over the dynamically accessible density range. For sake of comparison, we display in Fig. 3 an estimate of  $\xi_2$  evaluated from the pair correlation function  $g(r)$ , which, as is well known, changes only slightly with density. Note that in view of the small variation of all the static lengths,  $\xi_{\text{defect}}$ ,  $\xi_6$ ,  $\xi_2$  and  $\xi_p$ , trying to devise a crisper measuring procedure is unnecessary as it will not qualitatively alter the conclusions. Strikingly, the “dynamic length”  $\xi_{\text{dyn}}$  characterizing the spatial correlations in the dynamics and associated with dynamical heterogeneities is found to grow markedly over the same range of density. Whereas the change in the static length is measured in fractions of their low-density

value,  $\xi_{\text{dyn}}$  grows by a factor of almost 7 when reaching  $\phi = 0.59$  [14]. The diffusivity  $D$  and the structural relaxation time  $\tau$  meanwhile change by about 4 orders of magnitude (Fig. 3).

Although the above results may come as no surprise to those who believe the dynamical slowdown to be a purely kinetic phenomenon involving no growing static length scale, it is nonetheless worth checking whether one does not violate the bound between relaxation time and static correlation length put forward by Montanari and Semerjian [25],  $\tau \lesssim \tau_0 \exp(B \xi_{\text{PS}}^3)$ , where  $\tau_0$  is a constant setting the microscopic time scale. The coefficient  $B$  depends on density (or temperature for a glass-forming liquid) and is such that when  $\xi_{\text{PS}} \sim \sigma$  the right-hand side describes the “noncooperative dynamics” of the model [26]. For a hard-sphere fluid one then expects  $B \propto \beta P$  where  $P$  is the pressure. It should be stressed that the upper bound of  $\tau$  diverges with the pressure even in the absence of any growing  $\xi_{\text{PS}}$ , as when approaching  $T = 0$  for an Arrhenius temperature dependence. In the low and moderate density fluid, the relaxation time indeed follows  $\tau(\phi) \simeq \tau_{\text{low}}(\phi) = \tau_0 \exp[K \beta P(\phi)]$  with  $K$  a density-independent constant. One then finds that

$$\left( \frac{\log[\tau(\phi)/\tau_0]}{\log[\tau_{\text{low}}(\phi)/\tau_0]} \right)^{1/3} \lesssim \frac{\xi_{\text{PS}}(\phi)}{\xi_{\text{PS},0}}, \quad (2)$$

where  $\xi_{\text{PS},0}$  is the low-density limit of  $\xi_{\text{PS}}$ . Equation (2) thus provides a lower bound for the growth of a static length imposed by the dynamical slowdown.

To assess whether the above bound is satisfied or not, one needs an estimate of  $\xi_{\text{PS}}$ . The direct approach would be to consider the effect of pinning the boundary of a spherical cavity on the fluid inside, but one may reasonably expect that the penetration length studied above gives a rough estimate of  $\xi_{\text{PS}}$ . Near a random-first-order transition or near any first-order transition  $\xi_{\text{PS}} \sim \xi_p^3$  [27], but far from any transition, which is the case studied here, one expects  $\xi_{\text{PS}} \sim \xi_p$ . In any case, as seen in Fig. 3, the bound given by Eq. (2) increases only slowly in the dynamically accessible domain and is already satisfied by  $\xi_p$ . Note that this moderate growth of the bound further illustrates that hard spheres are not in fact very “fragile” in the regime up to  $\phi = 0.59$ , showing only a limited deviation with respect to the low-density behavior, which is in line with what is found for other simple fluids, such as the Lennard-Jones glass-forming liquids [28]. These observations may well correlate with the fact that most, if not all, 3D fluids of spherical particles are strongly frustrated in the sense discussed above.

These results indicate that the growth of a static length is not the controlling factor behind the relaxation slowdown in the range of density considered. This finding points to a mechanism for the slowdown that is either essentially “noncooperative”, or akin to that predicted by the mode-coupling theory [29, 30], where the

growth of a dynamic length is not accompanied by that of a static length. We cannot, however, draw any general conclusion on this question beyond this regime. In thermodynamic-based theories [7, 31], it is in this higher-density (or lower-temperature for a liquid) regime where cooperative behavior becomes dominant, and the dynamical slowdown is predominantly controlled by the growth of a static length. This regime is unfortunately mostly beyond present-day computer resources. A modest indication that a crossover takes place may, however, be given by the data for  $\xi_p$  and the bound, which both appear to display a steeper increase near  $\phi = 0.59$ .

In conclusion, we have shown that 3D hard spheres, like  $d > 3$  hard spheres and many other 3D simple glass formers, are too strongly frustrated for the dual picture in terms of defects to bring a useful simplification [5]. One may wonder if there exist other liquids with a different type of locally preferred order for which frustration is weaker and the picture can be put to work. Whereas this frustration regime can be achieved in 2D by curving space [10], no such example of simulation-accessible glass formers in 3D Euclidean space has yet been devised. In the regime accessed here, the static lengths are also found to grow very slowly, yet in a way that is compatible with the bound recently put forward between relaxation time and static length. This result further places serious doubts on the pertinence of local-order analysis in this dynamical regime for similar systems. The dynamic length increases significantly, which points instead to a decoupling between the increasingly heterogeneous character of the dynamics and its cooperative origin in terms of structural or thermodynamic quantities. A challenge would be to search for a possible crossover at still higher densities.

We acknowledge stimulating discussions with G. Biroli, C. Cammarota, D. R. Nelson, R. Mosseri and Z. Nussinov, and thank E. Zaccarelli for sharing configurations. This research was supported in part by the National Science Foundation Grant No. NSF PHY05-51164. BC received NSERC funding.

---

[1] G. Biroli *et al.* Nat. Phys. **4**, 771 (2008).  
[2] S. Karmakar, C. Dasgupta, and S. Sastry, Proc. Nat. Acad. Sci. U.S.A. **106**, 3675 (2009).  
[3] F. Sausset and D. Levine, Phys. Rev. Lett. **107**, 045501 (2011).  
[4] J.-F. Sadoc and R. Mosseri, *Geometrical Frustration* (Cambridge University Press, Cambridge, 1999).  
[5] D. R. Nelson, *Defects and geometry in condensed matter physics* (Cambridge University Press, New York, 2002).  
[6] D. B. Miracle, Nat. Mater. **3**, 697 (2004); H. Tanaka *et al.* Nat. Mater. **9**, 324 (2010); D. Coslovich and G. Pastore, J. Chem. Phys. **127**, 124504 (2007); C. L. Klix, C. P. Royall, and H. Tanaka, Phys. Rev. Lett. **104**, 165702 (2010); U. R. Pedersen, T. B. Schröder, J. C. Dyre, and

P. Harrowell, Phys. Rev. Lett. **104**, 105701 (2010).  
[7] G. Tarjus, S. A. Kivelson, Z. Nussinov, and P. Viot, J. Phys.: Condens. Matter **17**, R1143 (2005).  
[8] A. V. Anikeenko and N. N. Medvedev, Phys. Rev. Lett. **98**, 235504 (2007).  
[9] J. A. van Meel, B. Charbonneau, A. Fortini, and P. Charbonneau, Phys. Rev. E **80**, 061110 (2009).  
[10] F. Sausset, G. Tarjus, and P. Viot, Phys. Rev. Lett. **101**, 155701 (2008); F. Sausset and G. Tarjus, Phys. Rev. Lett. **104**, 065701 (2010).  
[11] The 4D simplicial hyperbolic tiling  $\{3, 3, 3, 6\}$  has  $|\sigma^2/R^2|$  larger than for the spherical tiling  $\{3, 3, 3, 4\}$ , while the hyperbolic tiling  $\{3, 3, 6\}$  has an infinite edge length.  
[12] F. C. Frank and J. S. Kasper, Acta Crystallogr. **11**, 184 (1958).  
[13] G. Brambilla *et al.* Phys. Rev. Lett. **102**, 085703 (2009).  
[14] E. Flenner, M. Zhang, and G. Szamel, Phys. Rev. E **83**, 051501 (2011).  
[15] The dense phase is the chromium boride crystal structure [32] or a fractionated crystal mixture, both of which rarely nucleate. The event-driven molecular dynamics simulations of 9888 particles (1236 for the overlap calculation) use a modified implementation of Ref. [33]’s; the structural analysis uses Ref. [34]’s tools.  
[16] E. Zaccarelli *et al.* Phys. Rev. Lett. **103**, 135704 (2009).  
[17] A. Okabe, B. Boots, K. Sugihara, and S. N. Chiu, *Spatial Tessellations: Concepts and Applications of Voronoi Diagrams* (Wiley, New York, 2000), Table 5.5.2.  
[18] H. S. M. Coxeter, *Introduction to Geometry* (John Wiley and Sons, New York, 1961).  
[19] P. J. Steinhardt, D. R. Nelson, and M. Ronchetti, Phys. Rev. B **28**, 784 (1983).  
[20] R. N. Ernst, S. R. Nagel, and G. S. Grest, Phys. Rev. B **43**, 8070 (1991).  
[21] L. Berthier and W. Kob, arXiv:1105.6203 (2011).  
[22] C. Cammarota and G. Biroli, arXiv:1106.5513 (2011).  
[23] P. Charbonneau and G. Tarjus, in preparation.  
[24] S. Karmakar, E. Lerner, and I. Procaccia, arXiv:1104.1036 (2011).  
[25] A. Montanari and G. Semerjian, J. Stat. Phys. **125**, 23 (2006).  
[26] S. Franz and G. Semerjian, in *Dynamical heterogeneities in glasses, colloids and granular materials*, edited by L. Berthier *et al.* (Oxford University Press, New York, 2011).  
[27] C. Cammarota, G. Biroli, M. Tarzia, and G. Tarjus, Phys. Rev. Lett. **106**, 115705 (2011).  
[28] M. Grousson, G. Tarjus, and P. Viot, J. Phys.: Condens. Matter **14**, 1617 (2002).  
[29] W. Götze, *Complex Dynamics of Glass-Forming Liquids*, International Series of Monographs on Physics, Vol. 143 (Oxford University Press, Oxford, 2009).  
[30] G. Biroli, J. P. Bouchaud, K. Miyazaki, and D. R. Reichman, Phys. Rev. Lett. **97**, 195701 (2006).  
[31] V. Lubchenko and P. G. Wolynes, Ann. Rev. Phys. Chem. **58**, 235 (2007).  
[32] J. K. Kummerfeld, T. S. Hudson, and P. Harrowell, J. Phys. Chem. B **112**, 10773 (2008); L. Filion and M. Dijkstra, Phys. Rev. E **79**, 046714 (2009).  
[33] M. Skoge, A. Donev, F. H. Stillinger, and S. Torquato, Phys. Rev. E **74**, 041127 (2006).  
[34] C. B. Barber, D. P. Dobkin, and H. Huhdanpaa, ACM Trans. Math. Softw. **22**, 469 (1996).